

# Cosmic rays at ultra high energies (Neutrinos!)

Markus Ahlers, Andreas Ringwald

*Deutsches Elektronen-Synchrotron DESY, Notkestr. 85, D-22607 Hamburg, Germany*

Huitzu Tu

*University of Southern Denmark, Campusvej 55, DK-5230 Odense M, Denmark*

---

## Abstract

Resonant photopion production with the cosmic microwave background predicts a suppression of extragalactic protons above the famous Greisen–Zatsepin–Kuzmin cutoff at about  $E_{\text{GZK}} \approx 5 \times 10^{10}$  GeV. Current cosmic ray data measured by the AGASA and HiRes Collaborations do not unambiguously confirm the GZK cutoff and leave a window for speculations about the origin and chemical composition of the highest energy cosmic rays. In this work we analyze the possibility of strongly interacting neutrino primaries and derive model-independent quantitative requirements on the neutrino-nucleon inelastic cross section for a viable explanation of the cosmic ray data. Search results on weakly interacting cosmic particles from the AGASA and RICE experiments are taken into account simultaneously. Using a flexible parameterization of the inelastic neutrino-nucleon cross section we find that a combined fit of the data does not favor the Standard Model neutrino-nucleon inelastic cross section, but requires, at 90% confidence level, a steep increase within one energy decade around  $E_{\text{GZK}}$  by four orders of magnitude. We illustrate such an enhancement within some extensions of the Standard Model. The impact of new cosmic ray data or cosmic neutrino search results on this scenario, notably from the Pierre Auger Observatory soon, can be immediately evaluated within our approach.

---

## 1 Introduction

In the mid-1960's Greisen [1], Zatsepin and Kuzmin [2] realized that the space-filling molasses of photons constituting the cosmic microwave background (CMB) limits the observation of high-energy charged particles originating at astrophysical sources. The attenuation length of protons within the CMB drops below 50 Mpc above the photo-pion production threshold of about  $E_{\text{GZK}} \approx 5 \times 10^{10}$  GeV. In the case of heavier nuclei, photo-disintegration with CMB photons predicts a similar and even stronger attenuation above this energy (e.g., [3]). Hence, the apparent horizon of charged ultra high energy (UHE) cosmic rays (CRs) is of size comparable with the diameter of our local supercluster. Accordingly, the contribution of extragalactic charged particles to the CR spectrum measured on Earth is expected to show a cutoff at  $E_{\text{GZK}}$ .

The UHE CR spectrum measured by the AGASA [4] and HiRes [5, 6, 7, 8] Collaborations is shown in Fig. 1. The reported flux estimates derived from UHE events show a qualitative difference between the data sets. While AGASA reports an excess of eleven events above  $10^{11}$  GeV, the HiRes data seem to support the exis-

tence of the GZK-cutoff. However, the significance of the difference is small due to the low statistics as well as large systematic errors in energy calibration. Apart from this, the origin and chemical composition of UHE CR remains a puzzle in astroparticle physics. The Pierre Auger Observatory (PAO), which will publish its first results in summer 2005, is expected to shed light on these questions.

A recent analysis of the HiRes data [9] indicates a change in the UHE CR composition at around  $10^{8.6}$  GeV from heavy nuclei to a light component, which can be interpreted as the onset of extragalactic proton dominance in the data. If this is correct the UHE CR data is expected to show a cutoff at  $E_{\text{GZK}}$  due to resonant photopion production in the CMB. This is shown as the thin shaded band in Fig. 1 for our model of extragalactic protons described in §2. On the other hand, this mechanism leads to the generation of high energy neutrinos from the decay of charged pions. This flux of *cosmogenic neutrinos* [10, 11] may exceed the proton flux above and around  $E_{\text{GZK}}$  depending on the particular model parameters. In general, these cosmogenic neutrinos are accompanied by neutrinos originating from photo-hadronic processes directly in the CR sources. Recently, two of us have been

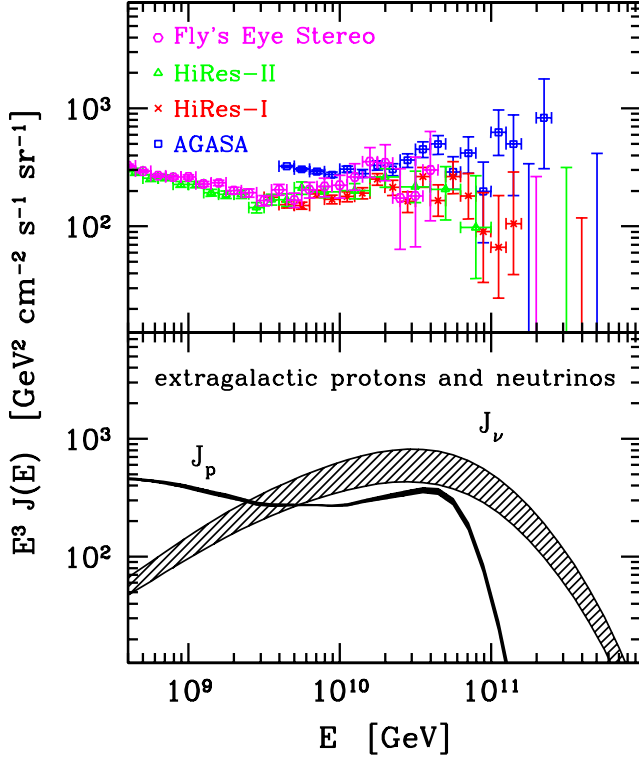


Fig. 1. *Top panel:* The quasi-vertical flux of UHE CRs measured by AGASA, Fly’s Eye and HiRes-I/II. *Bottom panel:* The shaded band shows the flux of extragalactic protons corresponding to the 90% CL of our fit. For the normalization we averaged the data between  $10^{8.6}$  GeV and  $10^{11}$  GeV according to the experimental exposure (see §2). The hatched band shows the combined flux of cosmogenic neutrinos and neutrinos from optically thin sources.

engaged in a derivation of a lower bound on this additional source of neutrinos directly related to the observed flux of CRs [12]. The sum of these two contributions is shown as the hatched band in Fig. 1.

The observation that the UHE cosmic neutrino flux may exceed the proton flux above  $E_{\text{GZK}}$  has motivated Berezhinsky and Zatsepin [10] to speculate on the possibility that neutrinos constitute the highest energy CR events, assuming them to interact so strongly as hadrons at the relevant energies [13]. Quantitatively, this requires a (rapid) rise of the neutrino-nucleon total inelastic cross section  $\sigma_{\nu N}^{\text{in}}$  by at least five orders of magnitude, above the Standard Model (SM) prediction,  $\sigma_{\nu N}^{\text{SM}} \approx 7.84 \text{ pb } (E_\nu/\text{GeV})^{0.363}$  [16, 17]. The realization of such a behavior has been proposed abundantly in scenarios beyond the (perturbative) SM: e.g. arising through compositeness [18, 19, 20], through electroweak sphalerons [21, 22, 23, 24, 25, 26, 27, 28, 29], through string excitations in theories with a low string and unification scale [30, 31, 32], through Kaluza-Klein modes from compactified extra dimensions [33, 34, 35, 36, 37, 38], or through  $p$ -brane production in models with warped extra dimensions [39, 40, 41],

respectively (for a recent review, see Ref. [42]).

Note that neutrino-nucleon inelastic cross sections are in general constrained by the search results on normal weakly-interacting UHE neutrinos. Up to now, UHE cosmic neutrinos have been searched for in the Earth atmosphere (Fly’s Eye/AGASA), in the Greenland (FORTE [43]) and Antarctic ice sheet (AMANDA [46]/RICE [44]), in the sea/lake (BAIKAL [47]), or in the regolith of the moon (GLUE [45]). For a given flux, the low if not zero search results so far can be turned into model-independent upper bounds on the neutrino-nucleon inelastic cross section in the energy range where  $\sigma_{\nu N}^{\text{SM}} \lesssim \sigma_{\nu N}^{\text{in}} \lesssim 0.05 - 0.5 \text{ mb}$  [48]. In strongly-interacting neutrino scenarios, this demands that the neutrino-nucleon inelastic cross section should pass very rapidly through this intermediate energy range. This constraint will be further strengthened with PAO’s search results on deeply-penetrating showers (see e.g. [48]), complemented by IceCube [49], ANITA [50] and possibly by EUSO [51], SaSA [52], and OWL [53].

In this work we present a general method, which was previously exploited in Ref. [28], to derive model-independent quantitative requirements on the cross section in strongly interacting neutrino scenarios. It exploits current CR data and UHE neutrino search results, and can easily incorporate or be applied to other data-releasing experiments, notably PAO. With this method the central question of the viability of strongly interacting neutrino scenarios can be addressed, confining the requirements on astrophysics (CR sources) and particle physics (inelastic  $\nu N$  cross section) simultaneously.

The outline of the paper is as follows. In §2 we calculate the incident fluxes of extragalactic protons and neutrinos assuming a power-like proton injection spectrum and a cosmic evolution of the source luminosity. The attenuation of the initial fluxes due to interactions with CMB photons and adiabatic energy losses are taken into account with the help of propagation functions. The number of neutrino-induced shower and cascade events measured at different zenith angles will depend strongly on the probability for neutrino scattering on target nucleons. The effect of a varying neutrino-nucleon inelastic cross section on the measurement by different type of experiments will be discussed in §3. In §4 we adopt a flexible parameterization for the rise of the inelastic neutrino-nucleon cross section with energy. This allows us to derive quantitative criteria on the viability of the strongly-interacting neutrino scenarios. In §5 we present our conclusions and give an outlook.

## 2 Extragalactic Particle Production

Following typical models of cosmic particle accelerators, such as active galactic nuclei or gamma ray bursts (see

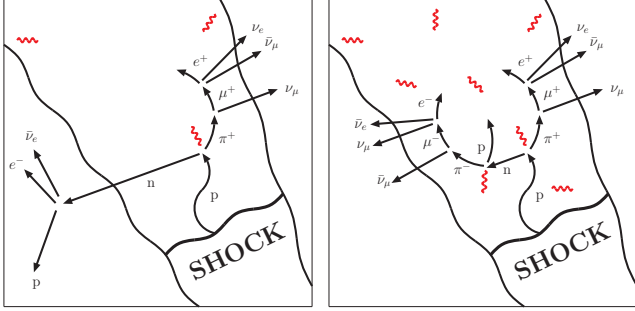


Fig. 2. Two possible production mechanisms of CRs by beam protons in a cosmic accelerator. The relative fluxes depend on the optical thickness of the magnetic confinement region.

e.g. [54] for a nice review), we assume that the origin of extragalactic protons are  $\beta$ -decayed neutrons, which are produced by photo-hadronic processes of beam protons and subsequently escape from the magnetically confined acceleration region. Fig. 2 shows a sketch of this mechanism. The relative output of other neutral particles, in particular high energy neutrinos, depend on the details of the source such as the densities of the target photons and the ambient gas [55]. In the following we will not be concerned about the detailed accelerator specifications and start directly with the injection spectrum of neutrons.

### 2.1 Extragalactic Protons

The apparent isotropy of the CR data suggests the assumption of a spatially homogeneous and isotropic distribution of the extragalactic neutron sources. Furthermore we assume that the emissivity distribution per co-moving volume  $\mathcal{L}_n$  factorizes into the red-shift evolution of the source luminosity and the injection spectrum. For simplicity we choose a widely used power-law ansatz with an exponential cut-off (see, e.g. Refs. [56, 57, 58, 59, 60]):

$$\mathcal{L}_n(z, E_n) \propto (1+z)^n E_n^{-\gamma} e^{-E_n/E_{\max}} \quad (1)$$

$z_{\min} < z < z_{\max}$

We exclude nearby (redshift  $z_{\min}$ ) and early ( $z_{\max}$ ) sources and fix these parameters in the following at  $z_{\min} = 0.012$  (corresponding to  $r_{\min} \approx 50$  Mpc) and  $z_{\max} = 2$ . The maximal injection energy  $E_{\max}$  is fixed at  $10^{12}$  GeV in our analysis.

The relevant flux of protons propagating towards the Earth resulting from the  $\beta$ -decay of the source neutrons is attenuated due to energy red-shift,  $e^+e^-$  pair production and photo-pion production with CMB photons (see e.g. [57, 58, 59]). The last of these processes provides the source of cosmogenic neutrinos. If we define  $P_{p|n}(E; E_n, r)$  as the expected number of protons above an energy  $E$  given a neutron with injection energy  $E_n$

at a distance  $r$ , then the expected proton flux incident on Earth can be expressed as

$$J_p(E) = \frac{1}{4\pi} \int_0^\infty dE_n \int_0^\infty dr \left| \frac{\partial P_{p|n}(E; E_n, r)}{\partial E} \right| \mathcal{L}_n. \quad (2)$$

The propagation functions  $P_{a|b}$  [61, 28] have been calculated using the SOPHIA Monte-Carlo program [62], and are available at [www.desy.de/~uhecr/](http://www.desy.de/~uhecr/). The propagation distance  $r$  and the redshift  $z$  are related by  $dz = (1+z)H(z)dr$ , where the Hubble expansion rate at a redshift  $z$  is related to the present one  $H_0$  through  $H^2(z) = H_0^2 [\Omega_M(1+z)^3 + \Omega_\Lambda]$ . Following recent results in cosmology [63] we will assume a flat  $\Lambda$ -dominated universe with relative energy densities  $\Omega_M = 0.3$  and  $\Omega_\Lambda = 0.7$  as well as  $H_0 = 72 \text{ km s}^{-1} \text{ Mpc}^{-1}$ , the center value of the Hubble Space Telescope Key project [64].

### 2.2 Cosmogenic Neutrinos and Neutrinos from Optically Thin Sources

Isospin and charge conservation requires that each neutron produced in photohadronic interactions of beam protons is accompanied by a charged pion. It decays and produces  $\nu_\mu, \bar{\nu}_\mu$  and  $\nu_e$ 's, as sketched in Fig. 2. On average, each neutrino carries about a quarter of the pion's energy. If we define  $\epsilon_\pi$  as the ratio  $E_{\pi^+}/E_n$  (see Ref. [65]) we can express the average energy of a single neutrino as  $E_\nu \approx \epsilon_\pi E_n/4$ . In the following we will use  $\epsilon_\pi \approx 0.28$ , suitable for resonant photoproduction at the energies in question (see Ref. [12]).

In optically thin sources the relative normalization of the neutron and neutrino emissivity is fixed by relating their bolometric fluxes per co-moving volume and is given by

$$\frac{\epsilon_\pi}{4} \mathcal{L}_\nu(z, \frac{\epsilon_\pi}{4} E_n) = 3 \mathcal{L}_n(z, E_n). \quad (3)$$

This flux of neutrinos is directly associated with the injected neutrons and serve as a minimal contribution from the source. In optically thicker sources neutrons may undergo photohadronic interactions before escaping the confinement region, as sketched in Fig. 2 (right). This will decrease the emissivity of neutrons compared to that of neutrinos. Depending on the ambient gas,  $pp$  interactions may also dominate over photohadronic processes in the source and produce additional neutrinos.

The opacity of the CMB to UHE protons propagating over cosmological distances guarantees a cosmogenic flux of neutrinos, originated in the reaction  $p + \gamma_{\text{CMB}} \rightarrow N + \pi^+ \rightarrow \mu^+ \nu_\mu \dots \rightarrow \nu_\mu \bar{\nu}_\mu \nu_e e^+ \dots$  [10]. Recently, two of us were involved in an investigation of the actual size of the cosmogenic neutrino flux [58]. In this work, we consider the combined flux of cosmogenic neutrinos and

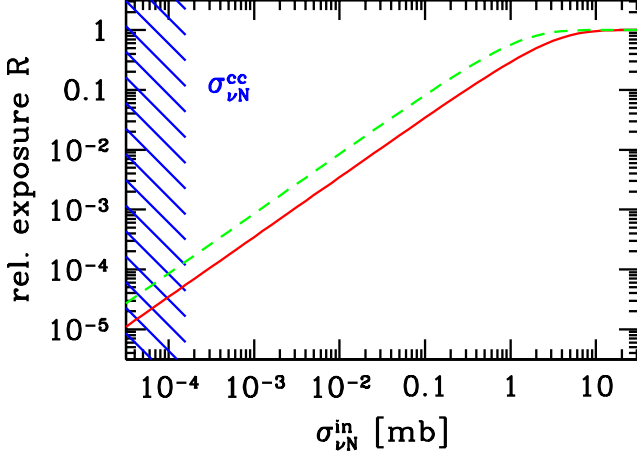


Fig. 3. Relative exposure  $\mathcal{R}$  (Eq. (5)) to strongly-interacting neutrinos as a function of the neutrino-nucleon inelastic cross section  $\sigma_{\nu N}^{\text{in}}$ , of AGASA (solid) and HiRes (dashed), respectively). The hatched region shows the predicted contribution from SM charged current interaction [16, 17].

neutrinos from  $p\gamma$  interactions in optically thin sources, which can be calculated by

$$J_{\nu}(E) = \frac{1}{4\pi} \sum_{n,\nu} \int_0^{\infty} dE_i \int_0^{\infty} dr \left| \frac{\partial P_{\nu|i}(E; E_i, r)}{\partial E} \right| \mathcal{L}_i, \quad (4)$$

where the propagation functions  $P_{\nu|n}$  and  $P_{\nu|\nu}$  are defined analogously to  $P_{p|n}$  in the previous section.

As it was discussed in Ref. [12] this flux of high energy neutrinos from optically thin sources is almost in reach of the AMANDA-II detector for neutrino energies of the order  $10^7$  GeV and should soon be observable by its successor experiment IceCube. This observation is crucial for our assumption about the sources of CRs and the associated flux of neutrinos from the same sources. If even cosmogenic neutrinos are not detected in future experiments, also the assumption on the extragalactic origin of CRs has to be reconsidered.

### 3 Footprints of Strongly Interacting Neutrinos

The search for UHE cosmic neutrinos is a challenging task due to their feeble interactions in the SM. To overcome this problem large-scale detectors and novel techniques are deployed and proposed. Up to now, experiments with UHE neutrino sensitivity include AGASA, RICE, GLUE, FORTE, BAIKAL, Fly's Eye, AMANDA, and PAO. Further ambitious projects include ANITA and IceCube, possibly followed by EUSO, SalSA, or OWL. However, if the neutrino-nucleon inelastic cross section  $\sigma_{\nu N}^{\text{in}}(E)$  increases more rapidly with energy than the SM predicts, UHE cosmic neutrinos could already leave their footprints in the CR observational data. This happens when the neutrino interaction

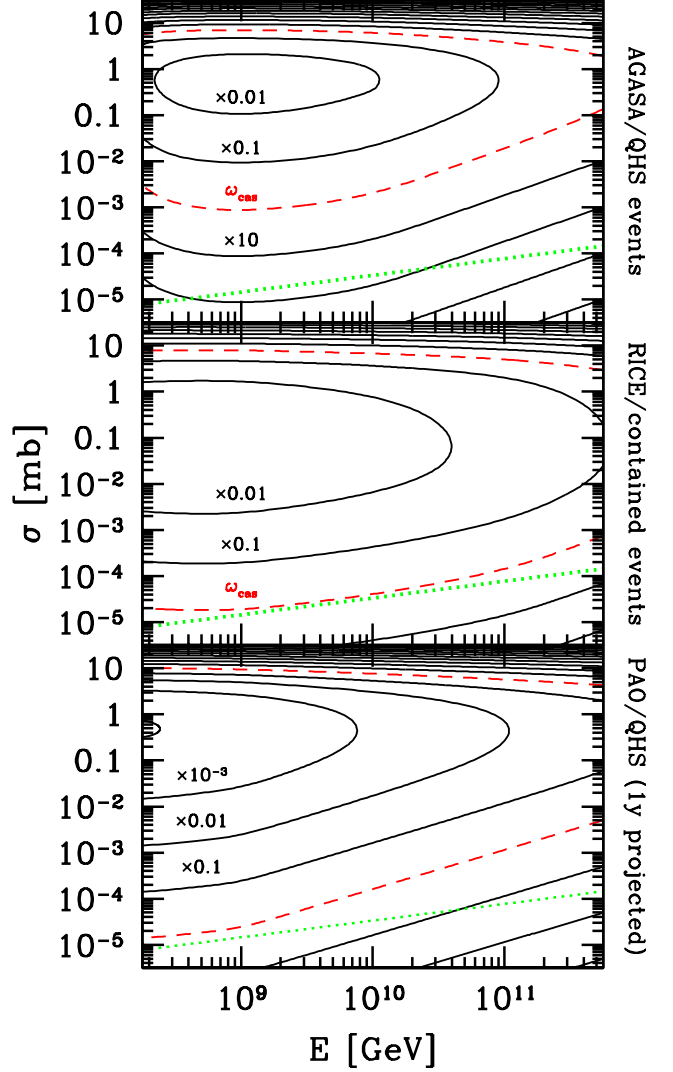


Fig. 4. The sensitivity in terms of the the maximal average flux  $J^{\text{max}}$  per bin  $\log_{10} \Delta E/E = \pm 0.05$ , with average cross section per bin  $\sigma$  consistent to the 95% C.L. with the experimental results on QHS events at AGASA (top), contained events at RICE (center) and QHS events at PAO (bottom). The flux is shown as  $E^2 J^{\text{max}}$  relative to the energy density  $\omega_{\text{cas}} = 8.5 \times 10^6 \text{ eV m}^{-2} \text{ s}^{-1} \text{ sr}^{-1}$  (dashed), corresponding to the cascade limit. The contours show the increase of the sensitivity by one order of magnitude (comp. the Appendices B, C and D). The dotted line is the extrapolation of SM charged and neutral current cross sections.

length  $\lambda_{\nu} \equiv m_p/\sigma_{\nu N}^{\text{in}}$  becomes comparable with the atmospheric depth  $x_{\text{atm}}(\theta)$  in the quasi-vertical direction, e.g.  $\theta \lesssim 45^\circ$  (cf. Appendix A).

In this work we aim to investigate the possibility of strongly interacting extragalactic neutrinos appearing as the highest energy CR events in dependence of a varying  $\sigma_{\nu N}^{\text{in}}(E)$ . We use CR data above  $10^{8.6}$  GeV measured by the AGASA and HiRes collaborations, and consider protons and neutrino primaries only. For simplicity we as-

sume that the characteristics of neutrino-induced showers are indistinguishable from those induced by protons. In particular, we assume for both primaries *i*) a complete conversion of the incident energy into the shower, and *ii*) equal detection efficiencies at the highest energies [67].

Under these assumptions we define  $\mathcal{R}(\sigma_{\nu N}^{\text{in}})$  as the relative experimental exposure to strongly interacting neutrinos compared to the exposure  $\mathcal{E}(E)$  to protons. The number of detected events is then given by

$$N_{\text{obs}} = \int dE \mathcal{E}(E) (J_p(E) + \mathcal{R}(\sigma_{\nu N}^{\text{in}}(E)) J_\nu(E)) . \quad (5)$$

The relative exposure  $\mathcal{R}(\sigma_{\nu N}^{\text{in}}(E))$  is determined by the search criterion on the zenith angle  $\theta$  and the (observed) atmospheric depth (cf. Appendix A and Fig. A.1) adopted by each experiments. HiRes ( $\theta \leq 60^\circ$ ) thus has a larger relative exposure than AGASA ( $\theta \leq 45^\circ$ ), as Fig. 3 shows. For both experiments one sees that neutrinos start to contribute significantly to quasi-vertical showers for  $\sigma_{\nu N}^{\text{in}} \gtrsim \mathcal{O}(1)$  mb. On the other hand, in the intermediate range  $\sigma_{\nu N}^{\text{SM}} \lesssim \sigma_{\nu N}^{\text{in}} \lesssim 1$  mb, neutrinos can still penetrate deeply in the quasi-horizontal direction, or in the ice upper surface. For a given neutrino flux, the non-observation of such events so far can be turned into model-independent upper bounds on the neutrino-nucleon inelastic cross section in the intermediate range, or be used to constrain models which predict an anomalously enhancement of  $\sigma_{\nu N}^{\text{in}}$  at high energies [48]. In the following we will focus on the search results on quasi-horizontal showers (QHS) at AGASA [68] and contained events at RICE [69]. Fig. 4 shows the sensitivity of these experiments in terms of the maximal average flux ( $J_\nu^{\text{max}}$ ) per bin and mean inelastic cross section ( $\sigma_{\nu N}^{\text{in}}$ ) consistent with the experimental results. For details of the calculation see Appendices B, C and D.

#### 4 High Energy Inelastic Neutrino-Nucleon Cross Section

For a satisfying explanation of post-GZK events by extragalactic neutrinos, the neutrino-nucleon cross section has to reach nucleonic values around  $E_{\text{GZK}}$  as shown in Fig. 3. In order to be consistent with the data on QHSs at AGASA and events at RICE one expects only steeply increasing inelastic interactions as good candidates for a combined statistical analysis. In the following we want to support these rather qualitative arguments by a statistical analysis of the existing data assuming strongly interacting extragalactic neutrinos.

In frequentists statistic the level of agreement of a particular hypothesis  $\mathcal{H}$  with the experimental data can be represented [70] by

$$\mathcal{G}(\mathcal{H}) = \sum_{N' | P(N') < P(N_{\text{exp}})} P(N' | \mathcal{H}), \quad (6)$$

Table 1

Best fit (81% CL), resolution of the fit, and range of parameters.

	$\gamma$	$n$	$\log_{10} \mathcal{A}$	$\log_{10} \frac{\Delta E}{E_{\text{th}}}$	$\log_{10} \frac{E_{\text{th}}}{1 \text{ GeV}}$
best fit	2.4	3.8	7.0	0.15	10.95
grid size	0.01	0.05	0.16	0.044	0.1
min	2.00	0.00	0.0	0.1	9.90
max	2.99	4.95	7.0	1.2	11.50

the integrated probability of those samples  $N'$  which have a smaller probability  $P$  than the actual experimental result  $N_{\text{exp}}$ . In general,  $\mathcal{H}$  is then accepted (or rejected) at a chosen significance level  $\mathcal{G}$  corresponding to a confidence level  $1 - \mathcal{G}$  [70]. As it is standard in statistics, we choose 90%, 95% and 99% as benchmarks for the acceptance of our model.

In our case, the probability  $P$  is made up by Poisson distributions of vertical events (AGASA, Fly's Eye Stereo and Hires-I/II; see Appendix A), QHSs at AGASA (see Appendix B) and contained events at RICE (see Appendix C) with an expectation value determined by the hypothesis  $\mathcal{H}$ . We also account in  $P$  for the systematic error in energy calibration of about 30% by a Gaussian distribution for a shift of the observed spectra by a multiple of the smallest bin-size. The expectation value for the Poisson-distributed events is determined by the hypothesis  $\mathcal{H}(\gamma, n, \sigma_{\nu N}^{\text{in}})$ , i.e. by the particular model for the inelastic neutrino-nucleon cross section  $\sigma_{\nu N}^{\text{in}}$  together with the source luminosity given by an injection index  $\gamma$  and an evolution index  $n$ .

The absolute value of the predicted flux is a priori unknown due to our lack of knowledge of the CR source luminosity. For each experiment individually we normalize the events induced by protons and neutrinos to the data between  $10^{8.6}$  GeV and  $10^{12}$  GeV. The resulting ambiguity in the normalization of the proton and neutrino fluxes has to be removed for a prediction of horizontal events at AGASA and contained events at RICE. In this

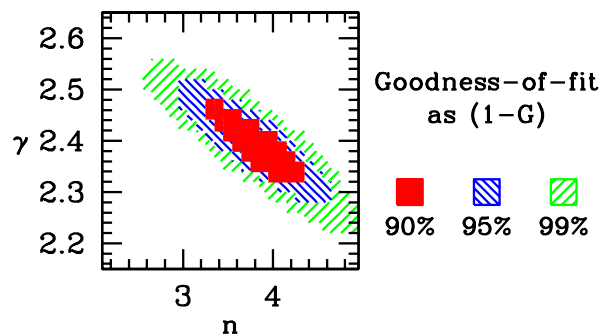


Fig. 5. The 90% (shaded), 95% (fine-hatched) and 99% (coarse-hatched) CLs of the injection spectrum marginalize w.r.t. the neutrino-nucleon cross section.



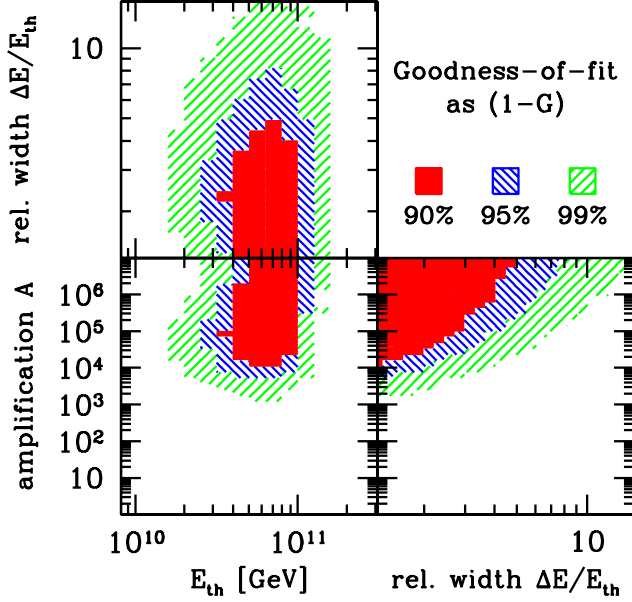


Fig. 6. The 90% (shaded), 95% (fine-hatched) and 99% (coarse-hatched) CLs of the  $\nu N$  cross section. We marginalize w.r.t. the other parameters.

case, we normalize the fluxes to an average data set interpolating between AGASA, Fly’s Eye and HiRes-I/II according to the exposure of the individual bins.

Now that we have set up our statistical analysis, we need to specify the particular neutrino-nucleon cross section for our hypothesis. There are various theoretical ideas for a rapid increase of the neutrino-nucleon cross section  $\sigma_{\nu N}$  referring to physics beyond the perturbative SM as was already stated in the introduction. Based on our previous considerations, we are interested in three characteristics of a strong neutrino–nucleon interaction:

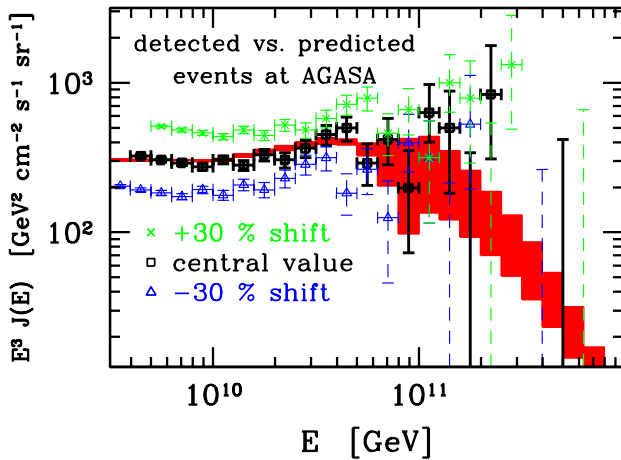


Fig. 7. The range of predicted events for AGASA induced by extragalactic protons and neutrinos corresponding to the 90% CL of the goodness-of-fit test (shaded band) compared to the AGASA data shifted in energy by  $\pm 30\%$ .

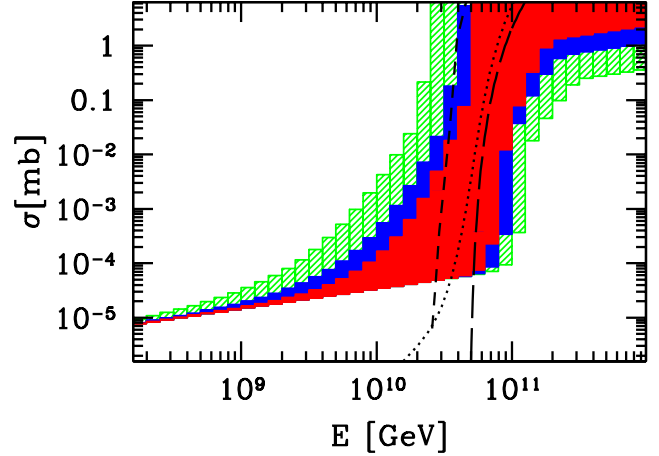


Fig. 8. The range of the cross section within the 99%, 95% and 90% CL. The lines are theoretical predictions of an enhancement of the neutrino-nucleon cross-section by electroweak sphalerons [29] (short-dashed),  $p$ -branes [41] (long-dashed) and string excitations [32] (dotted).

the threshold energy  $E_{\text{th}}$  marking the changeover from weak to strong interaction, the range  $\pm \Delta E/E_{\text{th}}$  for this change and the final amplification  $\mathcal{A}$  of the SM prediction  $\sigma_{\text{SM}}$  of charged and neutral current interactions. We parameterize the neutrino-nucleon cross section as

$$\log_{10} \left( \frac{\sigma_{\nu N}^{\text{in}}}{\mathcal{A} \sigma_{\text{SM}}} \right) = \frac{1}{2} \left[ 1 + \tanh \left( \frac{\ln(E_{\nu}/E_{\text{th}})}{\ln(\Delta E/E_{\text{th}})} \right) \right]. \quad (7)$$

The results of our goodness-of-fit test for the inelastic cross section (7) are shown in Figs. 5 and 6, with the best fit given in Table 1. Each plot of Fig. 5 and 6 shows the goodness-of-fit w.r.t. two parameters as confidence levels (CLs) of  $1 - \mathcal{G}$ . The remaining parameters of the set  $\{\gamma, n, \mathcal{A}, \Delta E/E_{\text{th}}, E_{\text{th}}\}$  are marginalized by a  $\chi^2$  minimization using simulated annealing as in Ref. [71].

Comparing the boundaries of the parameters in Table 1 with the contours in Fig. 6 it seems that the best fit is correlated to our choice of the maximal amplification  $\mathcal{A}$  and the minimal width  $\Delta E/E_{\text{th}}$ . For our statistical analysis we kept the relative width  $\Delta E/E_{\text{th}}$  always larger than 2 in order to account for the relative width of the bins of  $\geq 10^{0.1}$ . The relative exposure of strongly interacting neutrinos shown in Fig. 3 indicates that the contribution of neutrinos to the vertical spectrum saturates under an amplification of the inelastic cross section by more than seven orders of magnitude. This motivates us to limit the amplification below  $\mathcal{A} \leq 10^7$  in our analysis.

*The goodness-of-fit test of the combined data requires, to the 90% CL, a steep increase by an amplification factor of  $\mathcal{A} > 10^4$  over a tiny energy interval  $\Delta E/E_{\text{th}} < 5$  at around  $10^{11}$  GeV. In particular, the SM neutrino-nucleon inelastic cross section corresponding to  $\mathcal{A} = 1$  is not favored by the data.*

Fig. 7 shows the predicted events at AGASA as a shaded band corresponding to the 90% CL of the fit. The observed events at AGASA are shown together with a 30% shift of the energy to higher and lower values. The difference between the normalization of the AGASA and HiRes data can be removed by a relative re-calibration of the energy scale by 30% [72, 73]. In our approach we keep the normalization as stated from the AGASA and HiRes Collaborations and integrate the systematic error in energy calibration into Eq. (6).

For the 90%, 95% and 99% allowed range of the parameter shown in Fig. 6 we plot the range of the corresponding cross section in Fig. 8, which can be used as a *benchmark* test for scenarios proposing strongly interacting neutrinos as a solution to the GZK puzzle. As an illustration, we have considered three models of a rapidly increasing neutrino-nucleon cross section based on electroweak sphalerons [29],  $p$ -branes [41] and string excitations [32].

- *Electroweak sphalerons* : We have used the neutrino-nucleon cross section induced by electroweak instantons shown in Ref. [29], based on the neutrino-parton cross section from Ref. [27], the latter exploiting numerical results from Ref. [26]. A direct fit of  $\gamma$  and  $n$  with this cross section gives  $1 - \mathcal{G} = 98\%$ , which is in very good agreement with Fig. 8.
- *$p$ -branes* : We have calculated  $\sigma(\nu N \rightarrow \text{brane})$  given in Ref. [41] as Eqs. (9) and (10) for  $m = 6$  extra spatial dimensions, a fundamental scale of gravity  $M_D = 300$  TeV and a ratio  $L/L_* = 0.005$  of small to large compactification radii. We let all partons interact universally with the neutrino and use the CTEQ [74] Set 5D parton distribution functions (PDFs) contained in the FORTRAN library PDFLIB [75] Version 8.04 at the factorization scale  $\mu = 10$  TeV. Our fit of  $\gamma$  and  $n$  gives  $1 - \mathcal{G} = 83\%$ .
- *String excitations* : For the neutrino-quark cross section given in Ref. [32] with a string scale  $M_* = 70$  TeV and for the set of parameters  $N_0 = C = 16$ , characterizing the width and the absolute normalization, respectively (cf. their Fig. 2), we derived the neutrino-nucleon cross section with the PDFs described in the previous item. Our fit gives  $1 - \mathcal{G} = 84\%$  for this cross section, again in very good agreement with Fig. 8.

We should also mention at this point that a neutrino-nucleon cross section much larger than the SM predictions at some high energy scale will also have impact on the elastic scattering amplitude at much lower energies due to dispersion relations [76]. Eq. (E.2) in Appendix E gives the expected relative rise of the real amplitude

Table 2

Relative contribution to the real part of the scattering amplitude at  $E_\nu = 100$  GeV predicted by dispersion relations.

best fit	90% CL	95% CL	99% CL
0.091	$\leq 0.13$	$\leq 0.15$	$\leq 0.21$

compared to the SM prediction for arbitrary models of the neutrino-nucleon cross section. We have checked that for the models displayed in Fig. 8 there is no conflict with low energy data on elastic neutrino-nucleon scattering. Table 2 shows the maximal relative contribution of strongly interacting neutrinos to the real part of the elastic scattering amplitude predicted by the SM at  $E_\nu = 100$  GeV. For the 99% CL the maximal contribution is 21 %.

## 5 Conclusion and Outlook

We have shown that current data on the highest energy cosmic rays from AGASA and HiRes may be interpreted as the combined flux of extragalactic protons and strongly interacting extragalactic neutrinos. For the flux of neutrinos associated with neutrons from optically thin sources we derived requirements on the inelastic neutrino-nucleon cross section. We found, that a sufficiently steep increase of the cross section within one energy decade around  $E_{\text{GZK}}$  by four orders of magnitude may serve as a model also consistent with the search results on quasi-horizontal showers at AGASA and contained events at RICE. Our result is summarized in Fig. 8 where we show the range of the enhanced neutrino-nucleon cross section within the 90%, 95% and 99% CL of the fit. We have checked that the allowed region for the cross section is compatible with theoretical predictions, e.g. from electroweak sphalerons,  $p$ -branes and string excitations.

Our assumption of the extragalactic origin of the ultra high energy cosmic rays is motivated by experimental composition measurements. Standard mechanisms for the acceleration of these particles necessitates a *minimal* flux of extragalactic neutrinos associated with the observed CRs. If protons are produced in denser or optically thicker sources the flux of neutrinos is expected to be increased compared to the protons and the necessity of a strong inelastic cross section will be relaxed. This will also be the case if we extend the cut-off of the neutron injection spectrum  $E_{\text{max}}$  to values larger than  $10^{12}$  GeV, though this seems to be hard to achieve for astrophysical Bottom-Up sources (see e.g. [54] for a review). These ambiguities in the flux of UHE cosmic neutrinos will soon be clarified by future experiments such as IceCube [12].

The Pierre Auger Observatory will play a crucial role on models of strongly interacting neutrinos. Beside the spectrum of vertical showers with a much better statistic than AGASA and HiRes, the search of quasi-horizontal showers will soon have a stronger sensitivity to weakly interacting neutrinos as Fig. 4 indicates. Within our approach it will be easy to implement any future data, notably from Auger, which might finally reach large sensitivity on strongly interacting neutrino scenarios.

Here, also possible correlations with distant astrophysical sources can give a hint on neutrino primaries [77, 78].

## Acknowledgments

We would like to thank Luis Anchordoqui and Steen Hannestad for the nice discussions, and Zoltan Fodor and Sandor Katz for comments and for the support of our numerical analysis based on their original computer codes.

## A Observation of Vertical Showers at AGASA and HiRes

We start with the differential rate of air showers initiated at the point  $(\ell, \theta)$  by particles (cosmic ray protons, cosmic neutrinos etc.) incoming with energy  $E$  and of flux  $J(E)$ . Here,  $\ell$  is the distance of this point to the detector center measured along the shower axis, and  $\theta$  is the angle to the zenith at the point the shower axis hits the Earth's surface. We will focus in the following on showers with axis going through the detector. For detectors using the Fly's Eye technique this slightly underestimates the rate of induced event. However, for the relative exposure  $\mathcal{R}$  of strongly interacting neutrinos this should effect the results only for small cross sections, and then by a negligible amount.

The number of *induced* showers due to the inelastic interaction, the cross section for which is  $\sigma^{\text{in}}$ , per unit of length  $\ell$  along the shower axis, time  $t$ , area  $A_{\perp}$  perpendicular to the shower axis, shower energy  $E_{\text{sh}}$  and solid angle  $\Omega$  (with  $d\Omega = \sin \theta d\theta d\phi$ ) is

$$\frac{d}{d\ell} \left( \frac{d^4 N_{\text{ind}}}{dt dA_{\perp} d\Omega dE_{\text{sh}}} \right) = \frac{\rho_{\text{air}}[h(\ell, \theta)]}{m_p} \sigma^{\text{in}}(E) J(E) e^{-\frac{\sigma^{\text{in}}(E) x(\ell, \theta)}{m_p}}, \quad (\text{A.1})$$

where  $m_p$  is the proton mass, and  $\rho_{\text{air}}$  is the air density at the altitude  $h$ . The energy deposited in a visible shower is related to the incident particle energy by the inelasticity parameter, i.e.  $E_{\text{sh}} = yE$ . The distribution of  $y$  is dependent on the scattering process.

The number of showers *observed* is determined by the trigger efficiency  $\mathcal{P}(E, \theta)$  of the detector, and the range of atmospheric depths within which showers induced are visible to the detector. The latter, after carrying out the integral  $\rho_{\text{air}}(\ell, \theta) d\ell \equiv -dx$ , translates into a minimal and maximal atmospheric depth  $x_{-}(\theta)$  and  $x_{+}(\theta)$ , as shown in Fig. A.1. After integration along the line of

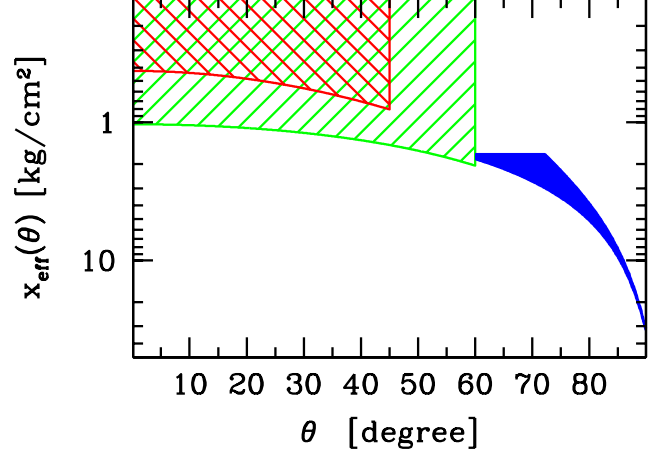


Fig. A.1. The range of atmospheric depths  $x_{-} < x_{\text{eff}} < x_{+}$  used for the calculation of Eq. (A.2) for quasi-vertical showers at AGASA (left-hatched) and HiRes (right-hatched) and quasi-horizontal showers at AGASA (shaded). For the quasi-vertical showers we use  $x_{-} \approx 0 \text{ kg cm}^{-2}$ .

sight of the observer, one has

$$\frac{d^4 N_{\text{obs}}}{dt dA_{\perp} d\Omega dE_{\text{sh}}} = \mathcal{P}(E_{\text{sh}}, \theta) J(E) \left( e^{-\frac{\sigma^{\text{in}}(E) x_{-}(\theta)}{m_p}} - e^{-\frac{\sigma^{\text{in}}(E) x_{+}(\theta)}{m_p}} \right). \quad (\text{A.2})$$

From this we can read off the experimental *exposure*  $\mathcal{E}(E)$  [ $\text{s m}^2 \text{ sr}$ ] defined as:

$$N_{\text{obs}} = \int dE \mathcal{E}(E) J(E). \quad (\text{A.3})$$

The AGASA and HiRes spectra shown in Fig. 1 have been observed in the quasi-vertical direction with  $\theta < 45^\circ$  and  $\theta < 60^\circ$ , respectively. In this angular range both detectors are sensitive to interactions in the outermost atmospheric layers and  $x_{-}(\theta)$  decreases to zero. The maximal atmospheric depth  $x_{+}(\theta)$  depend on the height of the detector sites and the line of sight observed in the atmosphere. Also, for the case of AGASA we reduce the total atmospheric depth  $x(\theta)$  by  $500 \text{ g cm}^{-2}$  in order to exclude those interactions too close to the detector site in order to be triggered [79]. Note that on average a  $10^{19} \text{ eV}$  shower develops to its maximum after traversing  $800 \text{ g cm}^{-2}$  in the atmosphere.

## B Quasi-horizontal Showers at AGASA

The AGASA Collaboration has observed one quasi-horizontal ( $\theta > 60^\circ$ ) shower (QHS) during an operation time of 1710.5 days with an expected background of  $1.72^{+0.14+0.65}_{-0.07-0.41}$  (MC statistics and systematics) [68]. The search criteria set the following constraints



on the shower maximum  $x_{\max}$ :  $x(\theta) - x_{\max}(\theta) < 500 \text{ g cm}^{-2}$  and  $x_{\max} \geq 2500 \text{ g cm}^{-2}$ . On average the shower develops its maximum after traversing  $800 \text{ g cm}^{-2}$  in the atmosphere. Hence the observed atmospheric depth shown in Fig. A.1 varies between  $x_-(\theta) = \max(1700 \text{ g cm}^{-2}, x(\theta) - 1300 \text{ g cm}^{-2})$  and  $x_+(\theta) = x(\theta)$ . The number of observed QHS events can then be calculated by Eq. (A.2). As the effective detector area for hadronic showers we took  $A = 56.1 \text{ km}^2$ . The horizontal detection efficiency  $\mathcal{P}_{\text{hor}}(E)$  for QHSs is reported to be 100% above  $10^{10} \text{ GeV}$  and approximately zero below  $10^8 \text{ GeV}$ . In between we use a power-law approximation  $\propto (\log_{10}(E/\text{GeV}) - 8)^n$ , which is fitted [80] to reproduce the upper bound of 3.52 events (95% CL) for the observation of one QHS from charged current interactions reported by the AGASA Collaboration. The upper plot in Fig. 4 shows the sensitivity of AGASA for QHSs in terms of the maximal neutrino flux  $E_\nu^2 J_\nu^{\max}(E_\nu)$  per flavor and per energy range  $\log_{10} \Delta E/E = \pm 0.05$  consistent to the 95% CL with the observation.

### C Contained Events at RICE

The Radio Ice Cherenkov Experiment (RICE) at the South Pole has searched for electro-magnetic and hadronic showers based on the principle of “radio coherence”. During an observation time of 3500 hours no candidate of an neutrino-induced event has been observed [69]. The expected number of events can be approximated as:

$$\frac{d^3 N}{dt d\Omega dE} = \frac{\rho_{\text{ice}}}{m_p} \int_{V_{\text{eff}}(E)} d\vec{r} J_\nu(E) \sigma_{\nu N}^{\text{in}}(E) e^{-\frac{\sigma_{\nu N}^{\text{in}} x(\vec{r}, \theta)}{m_p}} \quad (\text{C.1})$$

The effective detection volume  $V_{\text{eff}}(E)$  has been determined by MC simulations in [81]. We approximate the ice target as a cylinder with  $V_{\text{eff}}(E) = h\pi r^2(E)$  and a fixed height  $h = 1 \text{ km}$ . From this we can approximate the distance  $d(\vec{r}, \theta)$  a quasi-horizontal neutrino has to traverse in ice before it interacts with a nucleon inside the detector. Hence, the depth  $x(\theta)$  is composed of the atmospheric depth  $x_{\text{atm}}(\theta)$  and the depth in ice  $d(\vec{r}, \theta)\rho_{\text{ice}}$ . The sensitivity of RICE to the neutrino flux is shown as the center plot in Fig. 4.

### D Quasi-Horizontal Showers at PAO

The Pierre Auger Observatory (PAO), which is actually comprised of two sub-observatories, is the next large-scale neutrino detector in operation. The Southern site is currently operational and growing to its final size of  $\simeq 3000 \text{ km}^2$ .

The rate of neutrino-induced events at the ground arrays of PAO can be calculated using Eq. (A.2). The

effective aperture has been parametrized in Ref. [48] through a comparison with the geometric acceptance published in Ref. [82]. In short, to estimate the sensitivity for PAO, the following selection criteria were adopted: *i)*  $75^\circ \leq \theta \leq 90^\circ$  for the zenith angle, *ii)*  $X_{\max} \geq 2500 \text{ g cm}^{-2}$  for the shower maximum, which corresponds to requiring  $x_-(\theta) = 1700 \text{ g cm}^{-2}$  in this work. The altitude of the PAO Southern site (1200 m above sea level) was also taken into account in  $x_+(\theta) = x(\theta)$ . For hadronic showers with axis falling in the array, the effective area can then be parametrized as  $A_\perp(\theta, E) P(E)$ , with  $A_\perp(\theta, E) \approx \cos \theta \cdot 1.475 \text{ km}^2 (E/\text{eV})^{0.151}$ , and  $P(E) = 1$  for  $E \geq 10^{8.6} \text{ GeV}$ , while  $P(E) = 0.654 \log_{10}(E/\text{eV}) - 10.9$  below this energy. The effective aperture for all showers (i.e. including showers with axis not going through the array) is roughly 1.8 to 2.5 times larger, as shown in Ref. [82].

A first model-independent investigation of the sensitivity of PAO to anomalous neutrino interactions was performed in Ref. [48]. Assuming one year of operation with no event observed above the expected hadronic SM background (95% CL corresponding to 3.09 events), we estimate the prospects for PAO to strengthen the existing constraints imposed by AGASA and RICE. The 1-year projected sensitivity is shown in Fig. 4 (lowest panel).

### E Dispersion Relations

Regardless of a particular model, high energy cross section have to fulfill criteria relying on the analyticity and unitarity of the S-matrix. As was emphasized in [76] the total cross sections at high energies are constrained by low energy elastic amplitudes due to dispersion relations. One can relate the elastic scattering amplitude [83]  $\Re A$  to the principal value of an integral involving the total (anti-) neutrino-nucleon cross section  $\sigma^{\text{tot}} = \sigma^{\text{SM}} + \sigma^{\text{new}}$ :

$$\Re A(E_\nu) - \Re A(0) = \frac{E_\nu}{4\pi} \mathcal{P} \int_0^\infty dE' \left( \frac{\sigma_{\nu N}^{\text{tot}}(2m_p E')}{E'(E' - E_\nu)} + \frac{\sigma_{\bar{\nu} N}^{\text{tot}}(2m_p E')}{E'(E' + E_\nu)} \right) \quad (\text{E.1})$$

We assume that our high energy cross section obeys the Pomeranchuk theorem, i.e.  $\sigma_{\nu N}^{\text{new}} - \sigma_{\bar{\nu} N}^{\text{new}} \rightarrow 0$  for  $E_\nu \rightarrow \infty$ . The elastic amplitude at  $E_\nu \approx 0$  is dominated by Z-boson exchange of the order of  $G_F/2\sqrt{2}$ . For  $E_\nu \ll E_- \ll E_{\text{th}} - \Delta E$  we can use Eq. (E.1) to estimate the relative contribution of new physics at low energies as:

$$\frac{\Re A_{\text{new}}(E_\nu)}{\Re A_{\text{SM}}(E_\nu)} \approx \frac{\sqrt{2} E_\nu}{0.637 \pi G_F} \int_{E_-}^\infty dE' \frac{\sigma^{\text{SM}}}{E'} \frac{d}{dE'} \left( \frac{\sigma^{\text{tot}}}{\sigma^{\text{SM}}} \right) \quad (\text{E.2})$$

## References

- [1] K. Greisen, Phys. Rev. Lett. 16 (1966) 748.
- [2] G.T. Zatsepin and V.A. Kuzmin, JETP Lett. 4 (1966) 78.
- [3] M. Nagano and A.A. Watson, Rev. Mod. Phys. 72 (2000) 689.
- [4] M. Takeda et al., Astropart. Phys. 19 (2003) 447, astro-ph/0209422.
- [5] High Resolution Fly's Eye, D.J. Bird et al., Astrophys. J. 424 (1994) 491.
- [6] The High Resolution Fly's Eye, R.U. Abbasi et al., (2005), astro-ph/0501317.
- [7] R.U. Abbasi et al., Astropart. Phys. 23 (2005) 157.
- [8] Recent data from HiRes-I/II can be found at <http://www.physics.rutgers.edu/~dbergman/HiRes-Monocular-Spectra.html>.
- [9] High Resolution Fly's Eye, D.R. Bergman, (2004), astro-ph/0407244.
- [10] V.S. Beresinsky and G.T. Zatsepin, Phys. Lett. B28 (1969) 423.
- [11] F.W. Stecker, Astrophys. J. 228 (1979) 919.
- [12] M. Ahlers et al., (2005), astro-ph/0503229.
- [13] Along with the flux of cosmogenic neutrinos there will be a flux of cosmogenic photons from  $\pi^0$  decay. If the extragalactic magnetic field and the radio background are small, these photons might also contribute significantly to the UHE CRs [14, 15].
- [14] F.A. Aharonian, V.V. Vardanian and B.L. Kanevsky, Astrophysics and Space Science 167 (1990) 111.
- [15] G. Gelmini, O. Kalashev and D. V. Semikoz, arXiv:astro-ph/0506128.
- [16] R. Gandhi et al., Phys. Rev. D58 (1998) 093009, hep-ph/9807264.
- [17] J. Kwiecinski, A.D. Martin and A.M. Stasto, Phys. Rev. D59 (1999) 093002, astro-ph/9812262.
- [18] G. Domokos and S. Nussinov, Phys. Lett. B187 (1987) 372.
- [19] J. Bordes et al., (1997), hep-ph/9705463.
- [20] J. Bordes et al., Astropart. Phys. 8 (1998) 135, astro-ph/9707031.
- [21] H. Aoyama and H. Goldberg, Phys. Lett. B188 (1987) 506.
- [22] A. Ringwald, Nucl. Phys. B330 (1990) 1.
- [23] O. Espinosa, Nucl. Phys. B343 (1990) 310.
- [24] V.V. Khoze and A. Ringwald, Phys. Lett. B259 (1991) 106.
- [25] A. Ringwald, Phys. Lett. B555 (2003) 227, hep-ph/0212099.
- [26] F. Bezrukov et al., Phys. Lett. B574 (2003) 75, hep-ph/0305300.
- [27] A. Ringwald, JHEP 10 (2003) 008, hep-ph/0307034.
- [28] Z. Fodor et al., Phys. Lett. B561 (2003) 191, hep-ph/0303080.
- [29] T. Han and D. Hooper, Phys. Lett. B582 (2004) 21, hep-ph/0307120.
- [30] G. Domokos, S. Kovesi-Domokos and P.T. Mikulski, (2000), hep-ph/0006328.
- [31] G. Domokos et al., JHEP 07 (2001) 017, hep-ph/0011156.
- [32] W.S. Burgett, G. Domokos and S. Kovesi-Domokos, Nucl. Phys. Proc. Suppl. 136 (2004) 327, hep-ph/0409029.
- [33] G. Domokos and S. Kovesi-Domokos, Phys. Rev. Lett. 82 (1999) 1366, hep-ph/9812260.
- [34] S. Nussinov and R. Shrock, Phys. Rev. D59 (1999) 105002, hep-ph/9811323.
- [35] P. Jain et al., Phys. Lett. B484 (2000) 267, hep-ph/0001031.
- [36] M. Kachelriess and M. Plumacher, Phys. Rev. D62 (2000) 103006, astro-ph/0005309.
- [37] L. Anchordoqui et al., Phys. Rev. D63 (2001) 124009, hep-ph/0011097.
- [38] A.V. Kisselev and V.A. Petrov, Eur. Phys. J. C36 (2004) 103, hep-ph/0311356.
- [39] E.J. Ahn, M. Cavaglia and A.V. Olinto, Phys. Lett. B551 (2003) 1, hep-th/0201042.
- [40] P. Jain, S. Kar and S. Panda, Int. J. Mod. Phys. D12 (2003) 1593, hep-ph/0201232.
- [41] L.A. Anchordoqui, J.L. Feng and H. Goldberg, Phys. Lett. B535 (2002) 302, hep-ph/0202124.
- [42] Z. Fodor et al., (2004), hep-ph/0402102.
- [43] Fast On-orbit Recording of Transient Events satellite,  
A. R. Jacobson, S. O. Knox, R. Franz and D. C. Enemark, Radio Sci. **34**, 337 (1999).
- [44] Radio Ice Cerenkov Experiment,  
<http://www.bartol.udel.edu/~spiczak/rice/rice.html>
- [45] Goldstone Lunar Ultra-high energy neutrino Experiment,  
<http://www.physics.ucla.edu/~moonemp/public/>
- [46] <http://amanda.uci.edu/>  
M. Ackermann et al. [AMANDA Collaboration], Nucl. Phys. Proc. Suppl. **145**, 319 (2005).
- [47] V. Aynutdinov et al. [Baikal Collaboration], *Prepared for 28th International Cosmic Ray Conferences (ICRC 2003), Tsukuba, Japan, 31 Jul - 7 Aug 2003*
- [48] L.A. Anchordoqui et al., (2004), hep-ph/0410136.
- [49] IceCube,  
<http://icecube.wisc.edu/>
- [50] ANtarctic Impulse Transient Array,  
<http://www.ps.uci.edu/~anita/>
- [51] Extreme Universe Space Observatory,  
<http://www.euso-mission.org/>
- [52] Saldome Shower Array,  
P. Gorham et al., 2002, hep-ex/0108027.
- [53] Orbiting Wide-angle Light-collectors,  
<http://owl.gsfc.nasa.gov/>
- [54] D.F. Torres and L.A. Anchordoqui, Rept. Prog. Phys. 67 (2004) 1663, astro-ph/0402371.
- [55] K. Mannheim, R.J. Protheroe and J.P. Rachen, Phys. Rev. D63 (2001) 023003, astro-ph/9812398.
- [56] R.J. Protheroe and P.A. Johnson, Astropart. Phys. 4 (1996) 253, astro-ph/9506119.
- [57] R. Engel, D. Seckel and T. Stanev, Phys. Rev. D64

- (2001) 093010, astro-ph/0101216.
- [58] Z. Fodor et al., JCAP 0311 (2003) 015, hep-ph/0309171.
  - [59] D.V. Semikoz and G. Sigl, JCAP 0404 (2004) 003, hep-ph/0309328.
  - [60] V. Berezhinsky, A. Gazizov and S. Grigorieva, Nucl. Phys. Proc. Suppl. 136 (2004) 147, astro-ph/0410650.
  - [61] Z. Fodor and S.D. Katz, Phys. Rev. D63 (2001) 023002, hep-ph/0007158.
  - [62] A. Mucke et al., Comput. Phys. Commun. 124 (2000) 290, astro-ph/9903478.
  - [63] SDSS, M. Tegmark et al., Phys. Rev. D69 (2004) 103501, astro-ph/0310723.
  - [64] W.L. Freedman et al., Astrophys. J. 553 (2001) 47, astro-ph/0012376.
  - [65] E. Waxman and J.N. Bahcall, Phys. Rev. D59 (1999) 023002, hep-ph/9807282.
  - [66] L. Anchordoqui et al., Ann. Phys. 314 (2004) 145, hep-ph/0407020.
  - [67] For protons the reduction of the shower energy is negligible, i.e.  $E_{\text{sh}} = E_p$  (see Ref. [66])
  - [68] S. Yoshida et al., (2001), Prepared for 27th International Cosmic Ray Conference (ICRC 2001), Hamburg, Germany, 7-15 Aug 2001.
  - [69] I. Kravchenko, (2003), astro-ph/0306408.
  - [70] Particle Data Group, S. Eidelman et al., Phys. Lett. B592 (2004) 1.
  - [71] S. Hannestad, Phys. Rev. D61 (2000) 023002, astro-ph/9911330.
  - [72] D. De Marco, P. Blasi and A.V. Olinto, Astropart. Phys. 20 (2003) 53, astro-ph/0301497.
  - [73] D. De Marco and T. Stanev, (2005), astro-ph/0506318.
  - [74] <http://www.phys.psu.edu/~cteq/>
  - [75] H. Plothow-Besch, Comput. Phys. Commun. 75 (1993) 396.
  - [76] H. Goldberg and T.J. Weiler, Phys. Rev. D59 (1999) 113005, hep-ph/9810533.
  - [77] P. G. Tinyakov and I. I. Tkachev, JETP Lett. 74 (2001) 445 [Pisma Zh. Eksp. Teor. Fiz. 74 (2001) 499] [arXiv:astro-ph/0102476].
  - [78] P. G. Tinyakov and I. I. Tkachev, Astropart. Phys. 18 (2002) 165 [arXiv:astro-ph/0111305].
  - [79] D.A. Morris and A. Ringwald, Astropart. Phys. 2 (1994) 43, hep-ph/9308269.
  - [80] H. Tu, PhD thesis, DESY and University Hamburg, DESY-THESIS-2004-018, 2004.
  - [81] I. Kravchenko et al., Astropart. Phys. 20 (2003) 195, astro-ph/0206371, (We have used the non-LPM result shown as a dotted curve in Fig. 10 as an approximation for  $V_{\text{eff}}(E)$ . For energies larger than  $10^{11}$  GeV we approximate the volume as  $100 \text{ km}^3$ .).
  - [82] K.S. Capelle et al., Astropart. Phys. 8 (1998) 321, astro-ph/9801313.
  - [83] We do not consider helicity of the nucleos in the following.